1985ApJ...288L..11M

THE ASTROPHYSICAL JOURNAL, 288:L11–L15, 1985 January 1
© 1985. The American Astronomical Society. All rights reserved. Printed in U.S.A.

NEW MASER LINES OF METHANOL[1]

MASAKI MORIMOTO,[2] MASATOSHI OHISHI,[2,3] AND TOMIO KANZAWA[2]
Received 1984 June 14; accepted 1984 September 24

ABSTRACT

We found that the $4_{-1}-3_0$ *E* line (36.169 GHz) of methanol (CH_3OH) is a maser in Sgr B2, with an antenna temperature of up to 60 K and a velocity width of ~ 10 km s^{-1}. This maser is spatially extended with angular size of up to 90″, is distributed along the edge of H II regions, and apparently is not directly attached to star forming regions. Components with a narrow velocity width also exist. They are unresolved by our beam and have a velocity width of < 1.5 km s^{-1}.

We also discovered a new maser line of CH_3OH, the 7_0-6_1 *A* line (44.069 GHz) in Sgr B2, W51, and two other galactic sources.

These two maser lines have different radial velocities. Excitation study shows that these two lines can be inverted easily but require a kinetic temperature of > 80 K and a fractional abundance of methanol to molecular hydrogen of $\sim 10^{-7}$ for intense maser action.

Subject headings: interstellar: molecules — masers — nebulae: individual

I. INTRODUCTION

The compound CH_3OH is very abundant in molecular clouds and has many strong lines at centimeter- and millimeter-wave regions. This makes it a useful probe to study physical conditions within molecular clouds. In Sgr B2, Zuckerman *et al.* (1972) and Turner, Gordon, and Wrixon (1972) observed the $5_{-1}-4_0$ *E* line and $4_{-1}-3_0$ *E* line, respectively, and suggested from theoretical considerations that these transitions tend to be enhanced.

We observed the $4_{-1}-3_0$ *E* line using the NRO 45 m telescope and found that the line is very strong and is actually a maser. This *Letter* presents the results of the observations and preliminary results of the excitation study together with our discovery of another maser line of CH_3OH, 7_0-6_1 *A*.

Other lines known to be masing are $\Delta J = 0$, $\Delta K = 1$ *E* lines at 25 GHz in Ori KL (Barrett, Schwartz, and Waters 1971) and 9_2-10_1 *A* line at 23 GHz in W3(OH) (Wilson *et al.* 1984).

II. OBSERVATIONS

Observations were made on 1984 January 28 and February 1, with the 45 m telescope of Nobeyama Radio Observatory (NRO). The telescope has an aperture efficiency of about 55% and beam efficiency of about 80% at 40 GHz band and HPBW of 40″ and 50″ at the frequencies of two transitions (7_0-6_1 *A*: 44.069 GHz and $4_{-1}-3_0$ *E*: 36.169 GHz), respectively. The system noise temperature depended on weather and was typically 500 K (44 GHz) and 800 K (36 GHz) at the zenith. A bank of acousto-optical spectrometers (AOS), eight wide-band (AOS-W, 250 MHz bandwidth and 250 kHz resolution) and four high-resolution (AOS-H, 40 MHz bandwidth and 37 kHz resolution), were used.

Twenty-two points around the Sgr B2 H II region were observed in the two lines. Several other molecular lines were also observed simultaneously for comparison. We used position switching to remove baselines. One "OFF" position was observed after observing five different "ON" positions. At each position, the signal was integrated for 20 s, and typically 20 such cycles were repeated. The resulting rms noise fluctuation was 0.1 K for AOS-W and 0.3 K for AOS-H. Calibration of line intensity was made by the usual chopper wheel method.

Identifications of these lines with above mentioned transitions were due to Turner, Gordon, and Wrixon (1972) for the $4_{-1}-3_0$ *E* line and to a good agreement of radial velocity between that of the 7_0-6_1 *A* line and those of other methanol lines observed in Sgr B2.

III. RESULTS

Figure 1 shows sample profiles of $4_{-1}-3_0$ *E* line from three positions in Sgr B2. Position offset from map center is shown in the upper right of each profile (map center is $\alpha[1950.0] = 17^h44^m10^s.6$, $\delta[1950.0] = -28°22'05''$). They have very high intensities (T_A^* of up to 60 K) and large velocity widths (10–20 km s^{-1}). The profile consists of many velocity components of three distinct types: underlying thermal emission, strong and broad component, and very narrow component. They are referred to as thermal, broad, and spike components, respectively, and are indicated by arrows in the figure. Very high intensity of the broad components and very narrow velocity width of the spike components strongly suggest maser action in this line. The spike components have line widths typically less than 1.5 km s^{-1} and are not clearly visible in profiles taken with the AOS-W (frequency resolution of 250 kHz).

[1] This work was carried out under the common use observation program at the Nobeyama Radio Observatory (NRO). NRO, a branch of the Tokyo Astronomical Observatory, University of Tokyo, is a cosmic radio observing facility open for outside users.

[2] Nobeyama Radio Observatory.

[3] Department of Astronomy, University of Tokyo.

© American Astronomical Society • Provided by the NASA Astrophysics Data System

1985ApJ...288L..11M

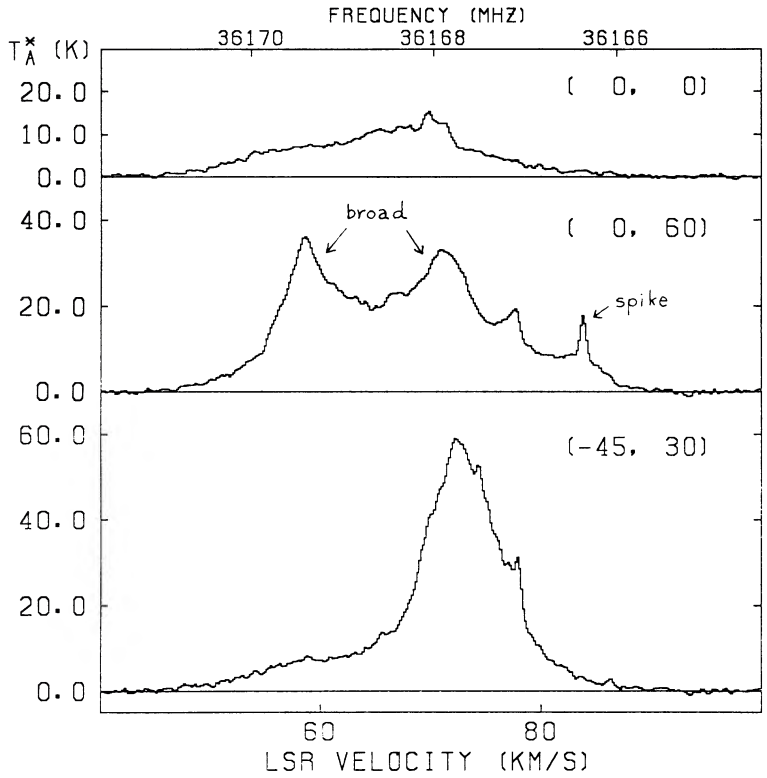

FIG. 1.—Sample profiles of the CH_3OH $4_{-1}-3_0$ E (36.16924 GHz) line in Sgr B2. Position of the map center is $\alpha(1950.0) = 17^h44^m10^s6$, $\delta(1950.0) = 28°22'05''$. Offset from map center is shown at the upper right by $(\Delta\alpha, \Delta\delta)$ in units of seconds of arc.

Behavior of the thermal component, where it is not contaminated by maser components, is very similar to that of other thermal molecular lines, and we will not treat them in detail here.

Figure 2 shows sample profiles of 7_0-6_1 A line in Sgr B2, W51, and two other galactic sources, G13.66−0.60 and G30.82−0.06 (through the courtesy of N. Ukita and M. Hayashi). These profiles all show narrow features. In particular, the former two sources show spikes as is the case with the $4_{-1}-3_0$ E line. The latter two sources were observed only with AOS-W (velocity resolution of ~ 3.5 km s^{-1}), and spikes would not have been resolved.

Distribution of maser components in Sgr B2 is shown in Figure 3 superposed on an H56α integrated intensity map which was obtained simultaneously with the $4_{-1}-3_0$ E line and represents the distribution of H II regions. Peak position, radial velocity, velocity width, peak antenna temperature T_A^*, and half-power size of these components are listed in Table 1.

We summarize the observed properties of the maser components as follows.

1. $4_{-1}-3_0$ E maser emissions are distributed along the edge of H II region, while 7_0-6_1 A masers lie closer to the center of the H II region. These two maser components have different radial velocities.

2. Broad components have typical source size of 60″–90″, velocity width of 10 km s^{-1}, and brightness temperature of 10–80 K. The luminosity is up to $\sim 10^{24}$ W.

3. Spike components are unresolved by our beam, and we estimate the source size of $< 10''$. Velocity width is typically less than 1.5 km s^{-1} in Sgr B2. We estimate a brightness temperature of > 200 K for the $4_{-1}-3_0$ E line and > 20 K for the 7_0-6_1 A line.

4. Maser components have a radial velocity of 70–80 km s^{-1} in the north and 50–60 km s^{-1} in the south. This general tendency is common to other molecular lines. But significant deviations from this trend exist; e.g., a broad component at (0″, 70″) has a radial velocity of 58 km s^{-1} and a spike component at (−50″, −10″) has a radial velocity of 80 km s^{-1}.

IV. DISCUSSION

a) *Are These Transitions Actually Maser Emission?*

The following facts indicate that the two transitions are actually masers.

Brightness of the Line.—The observed antenna temperature and the upper limit of the source size obtained of the spike component (Table 1) give a very high brightness temperature of higher than 200 K which is higher than the commonly accepted gas kinetic temperature of less than 100 K.

Velocity Width.—The velocity width of the spike component is about 1 km s^{-1} which is narrower by a factor of 10–20 than that of thermal emission observed in many molecular lines in Sgr B2. This is also the case in W51.

Intensity Relative to Other Molecular Lines.—We observed thermal lines of other molecules simultaneously (e.g., $J = 5-4$ and $J = 4-3$ lines of HCCCN). Line profiles of the two methanol transitions are very different from those of other molecular lines. The corresponding velocity components to

© American Astronomical Society • Provided by the NASA Astrophysics Data System

1985ApJ...288L..11M

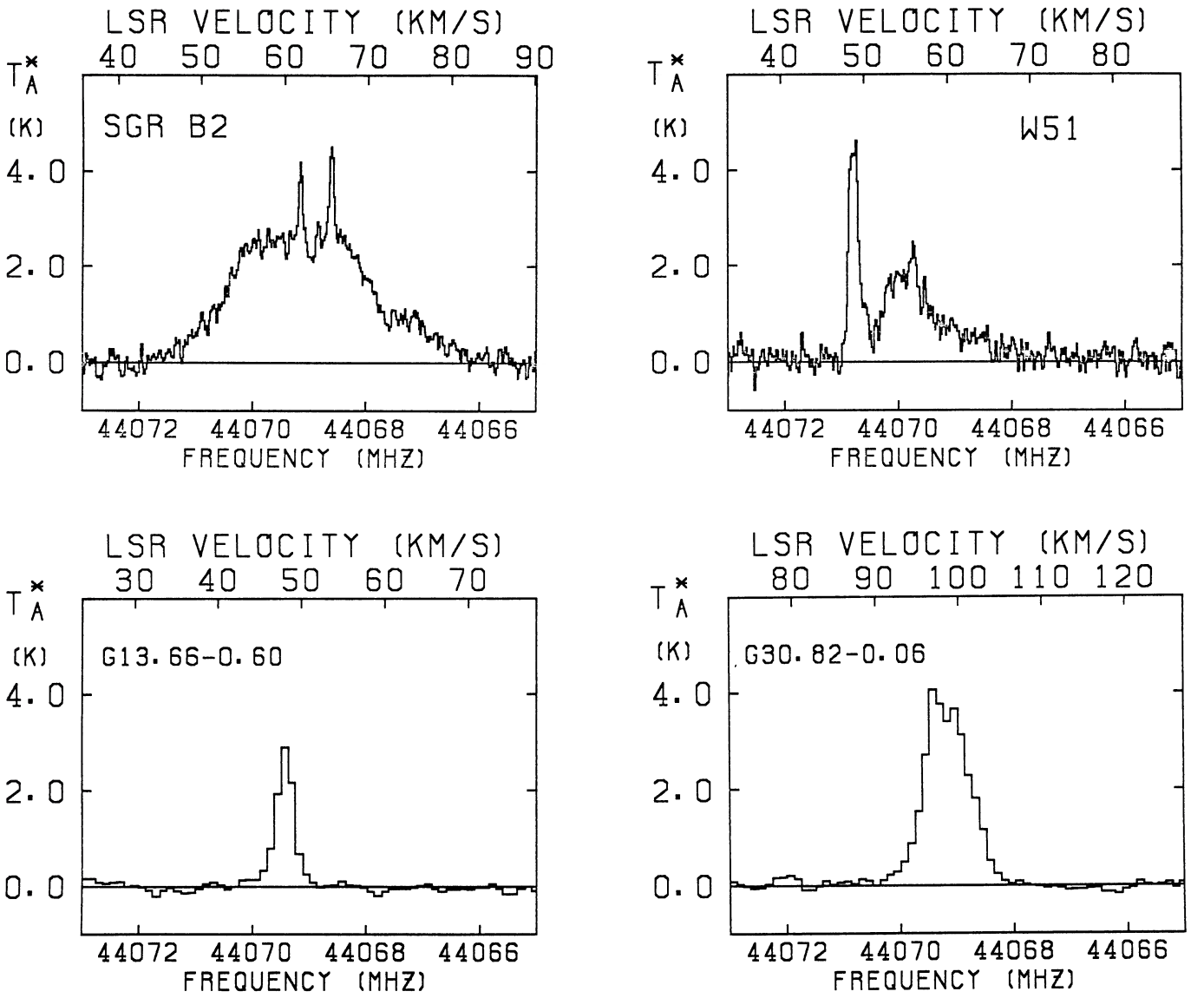

FIG. 2.—7_0–6_1 *A* maser lines in Sgr B2, in W51, G13.66−0.60, and G30.82−0.06. Profiles of Sgr B2 and W51 were taken with AOS-H, and the others were taken with AOS-W. Each axis at the bottom represents the rest frequency, and the one at the top represents the radial velocity with respect to the local standard of rest for each object.

CH_3OH spikes cannot be found on the profiles of other molecular lines. Moreover, for the 4_{-1}–3_0 *E* line, no other lines produce comparable antenna temperatures.

There is an alternative explanation for the spike components of methanol: these features could be due to quasi-thermal emission from clouds associated with small, dense, and hot (200 K) molecular cores. If such clouds existed, we would have expected to observe very strong and narrow emission lines from them in, for example, HCCCN lines observed simultaneously with methanol. These lines of other molecules, however, do *not* show any features corresponding to the spike components of the methanol lines. Thus this possibility is not the case.

The spike components show very anomalous excitation, and no possible identification other than masers is realistic.

The broad components represent a new type of maser. It is different from other "weak" masers in that the line is very broad, strong, and spatially extended.

b) *Excitation Conditions of Methanol*

We have made a statistical equilibrium calculation for the lowest 121 levels of CH_3OH *E* and *A* states, respectively, using the large velocity gradient model (Goldreich and Kwan 1974). Calculation was performed for $T_K = 40$, 80 K, $X(CH_3OH)/(dv/dr) = 5 \times 10^{-7}$ to $\sim 2.5 \times 10^{-11}$ (km $s^{-1}pc^{-1})^{-1}$, $n(H_2) = 10^3$ to 10^8 cm^{-3} by implicit Newton-Rafson method until the absolute value of the relative change in population for each level in two successive iterations became less than 0.1%. A spherically symmetric cloud was assumed.

© American Astronomical Society • Provided by the NASA Astrophysics Data System

1985ApJ...288L..11M

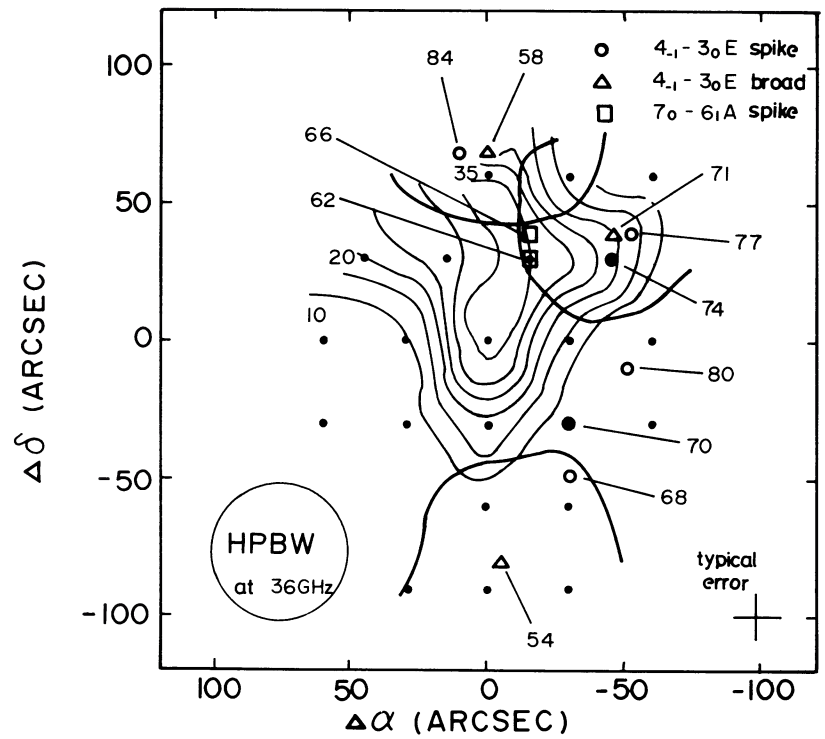

FIG. 3.—Distribution of CH_3OH maser emission superposed on H56α integrated intensity map which was observed simultaneously. The contour unit of the H56α map is K km s^{-1}. Observed points are indicated by dots (●). Spike components of the 4_{-1}–3_0 E, broad components of the 4_{-1}–3_0 E, and spike components of the 7_0–6_1 A line are denoted by circle, triangle, and square, respectively. Contours around broad components indicate the half-power size of each component. Radial velocity of each component is also shown. A cross bar at the bottom shows typical positional error. Position of the map center is as in Fig. 1.

TABLE 1

PROPERTIES OF MASER COMPONENTS

COMPONENT	PEAK POSITION Δα(″)	PEAK POSITION Δδ(″)	V_{LSR} (km s^{-1})	ΔV (km s^{-1})	T_A^* (K)	SIZE (arcsec)
4_{-1}–3_0 E (spike)	−30	−50	68	1.0	3.5	< 10
	−30	−30	70	1.5	9.8	< 10
	−45	+30	74	1.0	4.3	< 10
	−50	+40	77	1.7	9.4	< 10
	−50	−10	80	1.4	4.5	< 10
	+10	+70	84	1.2	11.4	< 10
4_{-1}–3_0 E (broad)	−5	−80	54	9.2	12.3	60 × 60
	0	+70	58	5.1	23.0	90 × 90
	−45	+40	71	6.6	58.0	90 × 90
7_0–6_1 A (spike)	−15	+30	62	1.7	1.9	< 10
	−15	+40	66	1.3	2.0	< 10

In the preliminary results, inferred brightness temperatures corresponding to spike components were reproduced for $T_K = 80$ K, $n(H_2) \approx 10^4$ cm^{-3}, $X(CH_3OH)/(dv/dr) \approx (1\text{–}5) \times 10^{-7}$ (km s^{-1}pc^{-1})$^{-1}$ for the 4_{-1}–3_0 E line and $n(H_2) \approx 10^4$–10^5 cm^{-3}, $X(CH_3OH)/(dv/dr) \approx 1 \times 10^{-7}$ (km s^{-1}pc^{-1})$^{-1}$ for the 7_0–6_1 A line. For $T_K = 40$ K, population inversion appeared; however, no transition had brightness temperature greater than 40 K. In this case, collisional excitation is not effective, and populations are mainly determined by radiative transitions. Then transitions between high-lying levels are optically thin, and no strong maser action occurs even if excitation temperature is negative. On the other hand, collisional excitation becomes rather effective at $T_K = 80$ K to populate high-lying levels, $|\tau|$ of 4_{-1}–3_0 E and/or 7_0–6_1 A line exceeds unity, and strong maser action is observed as a spike feature.

© American Astronomical Society • Provided by the NASA Astrophysics Data System

1985ApJ...288L..11M

The broad features have larger source sizes, and brightness temperature is not so high as that of spike features. Source sizes in Table 1 of these components give brightness temperature of typically less than 100 K. We obtained this result for lower fractional abundance of methanol ($\sim 10^{-7}$) and similar number density of molecular hydrogen. For this physical condition, the 7_0–6_1 *A* line has low brightness temperature of $\sim$ 10–20 K which is consistent with our observations.

Thus it is shown that a very high abundance of CH_3OH and a high kinetic temperature are necessary to explain the observed brightness temperatures.

As mentioned in the previous section, spike components of the 4_{-1}–3_0 *E* line and of the 7_0–6_1 *A* line have different radial velocities and different peak positions. This is explained from our calculation by the difference of excitation conditions in different portions of molecular cloud.

c) *Comparison with Other Maser Lines*

Both in Sgr B2 and W51, positions of CH_3OH maser sources do not coincide with those of other molecular masers (H_2O, OH: Genzel, Downes, and Bieging 1976; Genzel *et al.* 1979).

The 4_{-1}–3_0 *E* masers differ from previously known masers in many respects: they have large velocity widths; they are spatially extended; they are not directly attached to star forming regions or stellar envelopes; as shown in the previous section their pumping does not require special sources such as IR radiation, and in this respect they resemble weak masers in other molecules.

Perhaps the high abundance of CH_3OH causes the difference.

The luminosity is up to 10^{24} W for the 4_{-1}–3_0 *E* line and is an order of magnitude higher than those of OH and SiO masers but is much lower than that of some of H_2O masers in W49.

V. SUMMARY

We have detected two strong maser lines of CH_3OH in several sources. In Sgr B2, these maser lines emerge from warm and very high abundance regions of CH_3OH surrounding H II regions. The 4_{-1}–3_0 *E* masers have large velocity widths and are spatially extended. These characteristics are very different from those of previously known molecular masers. It is suggested that CH_3OH masers occur at the boundary between an H II region and a molecular cloud.

We wish to express special thanks to all the staff of Nobeyama Radio Observatory for their encouragement and help during this work. We are grateful to N. Kaifu for valuable discussions and suggestions. N. Ukita and M. Hayashi kindly permitted us to use methanol data prior to publication.

This work was supported in part by the Scientific Research Fund of the Ministry of Education (11271).

REFERENCES

Barrett, A. H., Schwartz, P. R., and Waters, J. W. 1971, *Ap. J. (Letters)*, **168**, L101.
Genzel, R., Downes, D., and Bieging, J. 1976, *M.N.R.A.S.*, **177**, 101P.
Genzel, R., *et al.* 1979, *Astr. Ap.*, **78**, 239.
Goldreich, P., and Kwan, J. 1974, *Ap. J.*, **189**, 441.
Turner, B. E., Gordon, M. A., and Wrixon, G. T. 1972, *Ap. J.*, **177**, 609.
Wilson, T. L., Walmsley, C. M., Snyder, L. E., and Jewell, P. R. 1984, *Astr. Ap.*, in press.
Zuckerman, B., Turner, B. E., Johnson, D. R., Palmer, P., and Morris, M. 1972, *Ap. J.*, **177**, 601.

TOMIO KANZAWA, MASAKI MORIMOTO, and MASATOSHI OHISHI: Nobeyama Radio Observatory, Nobeyama, Minamimaki-mura, Minamisaku-gun, Nagano 384-13, Japan

© American Astronomical Society • Provided by the NASA Astrophysics Data System